



Henslee, E., Torcal Serrano, R. M., Jabr, R., Fry, C., Hughes, M. D., Labeed, F. H., & Hoettges, K. F. (2016). Accurate quantification of apoptosis progression and toxicity using a dielectrophoretic approach. *Analyst*, 141(23), 6408-6415. DOI: 10.1039/C6AN01596D

Publisher's PDF, also known as Version of record

License (if available):  
CC BY-NC

Link to published version (if available):  
[10.1039/C6AN01596D](https://doi.org/10.1039/C6AN01596D)

[Link to publication record in Explore Bristol Research](#)  
PDF-document

This is the final published version of the article (version of record). It first appeared online via Royal Society of Chemistry at <http://pubs.rsc.org/en/Content/ArticleLanding/2016/AN/C6AN01596D#!divAbstract>. Please refer to any applicable terms of use of the publisher.

## University of Bristol - Explore Bristol Research

### General rights

This document is made available in accordance with publisher policies. Please cite only the published version using the reference above. Full terms of use are available:  
<http://www.bristol.ac.uk/pure/about/ebr-terms.html>



Cite this: *Analyst*, 2016, **141**, 6408

## Accurate quantification of apoptosis progression and toxicity using a dielectrophoretic approach†

Erin A. Henslee,<sup>a</sup> Ruth M. Torcal Serrano,<sup>a</sup> Fatima H. Labeed,<sup>a</sup> Rita I. Jabr,<sup>b</sup> Christopher H. Fry,<sup>‡b</sup> Michael P. Hughes\*<sup>a</sup> and Kai F. Hoettges<sup>§a</sup>

A loss of ability of cells to undergo apoptosis (programmed cell death, whereby the cell ceases to function and destroys itself) is commonly associated with cancer, and many anti-cancer interventions aim to restart the process. Consequently, the accurate quantification of apoptosis is essential in understanding the function and performance of new anti-cancer drugs. Dielectrophoresis has previously been demonstrated to detect apoptosis more rapidly than other methods, and is low-cost, label-free and rapid, but has previously been unable to accurately quantify cells through the apoptotic process because cells in late apoptosis disintegrate, making cell tracking impossible. In this paper we use a novel method based on light absorbance and multi-population tracking to quantify the progress of apoptosis, benchmarking against conventional assays including MTT, trypan blue and Annexin-V. Analyses are performed on suspension and adherent cells, and using two apoptosis-inducing agents. IC<sub>50</sub> measurements compared favourably to MTT and were superior to trypan blue, whilst also detecting apoptotic progression faster than Annexin-V.

Received 14th July 2016,  
Accepted 16th October 2016

DOI: 10.1039/c6an01596d

www.rsc.org/analyst

## Introduction

The study of apoptosis, or programmed cell death, is of great significance because it plays an important role in the normal development of multi-cellular organisms. Problems with the regulation of apoptosis can lead to diseases such as cancer (too little apoptosis) or neurodegenerative conditions such as Parkinson's or Alzheimer's diseases (too much apoptosis). New compounds that regulate apoptotic pathways can have applications as therapeutic agents, and hence quantifying the effectiveness of the new compounds is essential in drug discovery. Apoptotic cell death has a distinct cytological morphology and the signalling cascade is regulated at several points, therefore, there are many methods and opportunities to evaluate apoptotic death. There are several assays for apoptosis detection and understanding the mode of operations, their pros and cons, as well as the limitations of each assay is

important. The process of apoptotic cell death can be completed in a few hours, and therefore if the assay is performed too early or too late, the results may not be accurate. Of the methods used to study apoptosis, spectroscopic techniques are standard, though new options are emerging.<sup>1</sup> Most spectroscopic techniques for apoptosis rely on fluorescence detection of immunochemical labels or fluorescent probes which react to the cell environment during apoptosis. There are several options available including Annexin V staining, the TUNEL assay, and measurement of mitochondrial membrane potential.<sup>1</sup> These assays measure different parameters which correlate with apoptotic progression. Trypan blue inclusion in cells measures surface membrane integrity by assessing the number of cells that will allow trypan blue to enter the cell interior. The MTT assay is a colourimetric assay to assess cell metabolic activity, as viable cells with an active metabolism convert MTT into a purple coloured formazan product. The TUNEL assay detects DNA fragmentation by labelling the terminal end of nucleic acids and such DNA fragmentation is a characteristic hallmark of apoptosis. The Annexin-V assay measures the loss of phospholipid asymmetry in the cell membrane which occurs early in the apoptotic process; phosphatidylserine, which is usually in the inner membrane leaflet, is transported to the outer leaflet as an "eat me" signal to macrophages;<sup>2</sup> fluorescence labelling of Annexin V, combined with a nuclear stain, allows distinguishing between healthy, early apoptotic and late apoptotic cells using flow cytometry.<sup>3</sup> The early apoptotic phase can be quite brief, and so experiments at

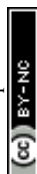
<sup>a</sup>Centre for Biomedical Engineering, Department of Mechanical Engineering Sciences, University of Surrey, Guildford, Surrey GU2 7XH, UK. E-mail: m.hughes@surrey.ac.uk

<sup>b</sup>Faculty of Health and Medical Sciences, University of Surrey, Guildford, Surrey GU2 7XH, UK

†Electronic supplementary information (ESI) available. See DOI: 10.1039/c6an01596d

‡Present address: School of Physiology and Pharmacology, University of Bristol, University Walk, Bristol BS8 1TD, UK.

§Present address: Department of Electrical Engineering and Electronics, University of Liverpool, Brownlow Hill, Liverpool L69 3GJ, UK.



different drug incubation times must be performed to prove that cells exhibit early apoptosis before reaching late apoptosis/necrosis. Whilst Annexin is fairly robust when used in suspensions growing cells, the use of flow cytometry can produce anomalous results due to damage caused by shear forces.<sup>4</sup>

In addition to indicating the presence or absence of apoptosis in the cell population, new compounds need to be quantified in their effectiveness or cytotoxicity. In most cases this is measured using the half maximal inhibitory concentration (IC<sub>50</sub>), which indicates the necessary drug concentration to inhibit a biological process on a cell population by half. There are various types of tests that are typically used to determine the IC<sub>50</sub> of a drug including simple light microscopy such as viability measures with trypan blue, fluorescent microscopy, 3-(4,5-dimethylthiazol-2-yl)-2,5-diphenyltetrazoliumbromide (MTT) assay,<sup>5</sup> and characterising cell populations through flow cytometry.<sup>6</sup> All of these methods involve staining of the cells often with expensive and cytotoxic dyes, lengthy preparation procedures, and rely on cellular events that occur as a result of drug exposure downstream of the initial drug effect. There is also the added complexity of comparing methods, as each measures viability mechanistically.

Dielectrophoresis (DEP) has been used as an alternative method of analysing the onset of apoptosis in the past, having been used to detect changes in cell phenotype within 30 minutes of drug incubation.<sup>7</sup> DEP was first demonstrated to be capable of detection physiological changes in apoptosis in 2002,<sup>8</sup> when Wang *et al.* demonstrated that the technique could more sensitively detect apoptotic induction than common methods such as the Annexin-V assay, using cross-over methods to study changes in the cell membrane. Subsequent work compared DEP and Annexin-V for both membrane and cytoplasm, and found that DEP could detect apoptosis considerably earlier than the conventional test for PS expression in K562 cells, and that early events in apoptosis such as the calcium activated translocation of the negatively charged phospholipid phosphatidylserine (PS) and the reduction of intracellular potassium all precede membrane degradation and thus detection by methods such as trypan blue or MTT.<sup>8-14</sup> More recent work has used the detection of apoptosis as a test for new DEP-based cytometry and cell sorting devices;<sup>15-20</sup> in all cases, devices were presented that were able to sort apoptotic from non-apoptotic cells, indicating again that apoptosis can be measured according to changes in cell electrophysiology.

Whilst DEP has been conclusively shown to be able to discriminate between apoptotic and non-apoptotic cells, analyses have thus far been based on the analysis of intact cells in the early stages of apoptosis. In fact, a key stage in the apoptotic progress is the disintegration of the cell into apoptotic bodies, which cannot be detected by most DEP methods, preventing DEP from accurately quantifying apoptosis progression across a population. This is significant, because whilst DEP can be used to identify whether a given cell is apoptotic or not, it is significantly more difficult to quantify apoptosis across a population in order to assess, for example, the concentration of a drug

required to induce apoptosis (the IC<sub>50</sub>); such a measurement would require the detection and quantification of apoptotic bodies (typically 1 μm across) as well as intact cells.

In this paper, we use a DEP analysis technique which analyses light absorbance changes due to DEP, hence allowing the quantification of apoptotic bodies. The DEP method was benchmarked with a suspension cell line (Jurkat) and the widely-used anti-cancer drug doxorubicin (DOX). Then, two studies were carried out on HeLa (adherent) and Jurkat (suspension) cells to benchmark DEP's speed and accuracy against MTT, trypan blue and flow cytometry with Annexin V/PI for apoptosis. The work demonstrates that with appropriate preparation, DEP analysis is as accurate as existing techniques whilst also being faster, simpler and cheaper to perform.

## Experimental methods

### Cell culture

Jurkat cells were cultivated in modified RPMI-1640 medium (Biosera, UK) supplemented with 10% heat-inactivated foetal bovine serum (Invitrogen, UK), 2 mM L-glutamine and 1% penicillin-streptomycin (Sigma-Aldrich, UK) and sub-cultured every 48 h.

HeLa cells were cultivated in MEM with Earle's salts and non-essential amino acids (Biosera, UK) supplemented with 10% heat-inactivated foetal bovine serum (Invitrogen, UK), 2 mM L-glutamine and 1% penicillin-streptomycin (Sigma-Aldrich, UK). The medium was changed every 48 h and the cells were passaged using Accutase® (Sigma-Aldrich, UK) at around 70% confluence. HeLa cells were seeded at 6000 cells per cm<sup>2</sup> in T175 flasks.

### Drug treatments and preparation

**Preparing mixtures.** Jurkat cells were incubated with a high dose (10 μM) of doxorubicin hydrochloride (DOX, Sigma-Aldrich, UK) for 16 h. This incubation was optimized to provide a control sample where 100% of cells had been affected by DOX.

To prepare cells for the DEP assay, samples were centrifuged at room temperature at 259g for 6 minutes and washed in iso-osmotic DEP medium consisting of 8.5% (w/v) sucrose, 0.5% (w/v) dextrose, 100 μM CaCl<sub>2</sub> and 250 μM MgCl<sub>2</sub><sup>21</sup> adjusted to a conductivity of 0.01 Sm<sup>-1</sup> using phosphate-buffered saline (PBS), and resuspended at a final cell concentration of 10<sup>6</sup> cells per ml (±15%). To calibrate how well DEP detects different sub-populations in a homogenous sample, a sample of healthy cells (not treated with DOX) and a sample of DOX-treated cells were prepared for DEP experiments. Then ratios of the healthy and the treated cell samples were prepared in ratios of 1 : 3, 2 : 2 and 3 : 1. A viability test was carried out on 20 μL of each of the mixtures as well as on the original samples using trypan blue 0.4% solution.

**Cytotoxicity measurement.** Staurosporine solution (1 mM in DMSO) from *Streptomyces* sp. (Sigma-Aldrich, UK) was used to induce apoptosis. A treatment of 1 μM staurosporine (Sigma-Aldrich, UK) was added to the HeLa flasks 24 h after seeding,



in order to ensure exponential growth. Cells were incubated for 0.5 h, 2 h and 4 h. Before DEP experiments, the drug treatment was terminated by centrifuging, removing the supernatant and resuspending in DEP media. Healthy HeLa cells attach to the flask, whereas dying cells lose their ability to attach and float in the culture medium. After treatment with staurosporine, supernatants containing detached apoptotic cells were transferred to new tubes. The remaining cells were detached following incubation with Accutase® which has been shown to not significantly alter the DEP properties of the cells.<sup>22</sup> These cells were then centrifuged at room temperature at 259g for 6 minutes. The supernatant was removed and the pellets were resuspended in the previously-described experimental medium. The final cell population was adjusted for DEP measurements to  $1.15 \times 10^6$  cells per ml ( $\pm 15\%$ ).

**IC<sub>50</sub> measurement.** Doxorubicin (Sigma-Aldrich, UK) was dissolved in sterile filtered distilled water, to achieve a 1.72 mM stock solution, aliquoted, and kept at 4 °C. Jurkat cells were treated with 0.1, 0.3, 0.5 or 1 μM doxorubicin (DOX) 24 h after the previous passage to ensure exponential growth. Cells were incubated with different doses of DOX for 8, 16 or 32 h before the drug treatment was terminated. Each of these samples was centrifuged at room temperature at 259g for 6 minutes in experimental medium, resuspended to a final cell concentration of  $10^6$  cells per ml ( $\pm 15\%$ ).

### DEP assay

The DEP assays were conducted on a DEPTech 3DEP well-based DEP cytometer<sup>23–25</sup> (Uckfield, UK). The instrument (Shown in Fig. 1) uses twenty parallel 3D electrode arrays to infer the DEP behaviour of a cell population by analysing the radial motion of cells within the well over a period of 10 seconds. It can measure the DEP response reliably up to 45 MHz, providing more accurate information about the dielectric properties of the cytoplasm.

Approximately 80 μL of prepared cell suspension was pipetted into a 3DEP disposable chip, inserted into the reader and energized at 10 kHz–20 MHz to produce a full DEP spectrum. This was repeated for each treatment group at least 5 times. Data were analysed over 10 s (Jurkat) or 40 s (HeLa) intervals.



**Fig. 1** Two DEPTech 3DEP cell analysers; the device on the left of the image is closed (as when in use), the device on the right is open to show the chip (red) and optical path.

A single shelled model<sup>26,27</sup> was fitted to the average of the sample data using the averages of measured cell radii.

The effective permittivity and conductivity of the particle considering a single shell model is given by:

$$\epsilon_p = \epsilon_m \frac{\gamma^3 + 2 \left( \frac{\epsilon_c - \epsilon_m}{\epsilon_c + 2\epsilon_m} \right)}{\gamma^3 - \left( \frac{\epsilon_c - \epsilon_m}{\epsilon_c + 2\epsilon_m} \right)} \quad (1)$$

$$\sigma_p = \sigma_m \frac{\gamma^3 + 2 \left( \frac{\sigma_c - \sigma_m}{\sigma_c + 2\sigma_m} \right)}{\gamma^3 - \left( \frac{\sigma_c - \sigma_m}{\sigma_c + 2\sigma_m} \right)} \quad (2)$$

where  $\gamma = R/(R - d)$ ;  $R$  is the particle radius;  $d$  is the cell membrane thickness;  $\epsilon_c$ ,  $\sigma_c$  and  $\epsilon_m$ ,  $\sigma_m$  are the complex permittivities and conductivities of the cytoplasm and the membrane, respectively.

Broche *et al.* developed a mathematical method to model multiple sub-populations within a sample.<sup>28</sup> This is achieved by adding together the individual single-shell models of each subpopulation at each frequency point. MATLAB (The MathWorks, Inc., Natick, MA) was used to establish Pearson correlation coefficients ( $R$ ) and RMS errors of the final multi-population fits. All data presented here have  $R$ -values  $> 0.99$ . Cell radii were obtained by image analysis of cells on a haemocytometer using Image-J (National Institute of Health, Maryland, US). One hundred cells were measured for each sample. The distribution of cell size was analysed using SPSS (SPSS Inc. Chicago, IL).

### Flow cytometry measurements

Annexin V FITC Apoptosis detection kit (Sigma-Aldrich, UK) was used to detect apoptosis using flow cytometry. HeLa cell concentration was adjusted to  $10^6$  cells per ml. Staurosporine treatment was applied to the wells at: 0.5 h, 2 h, and 4 h. A control of non-induced HeLa cells for a zero time point was also established. After the drug treatment was terminated, the cells were brought into suspension and washed twice with PBS. Control cells were also seeded in order to use them for compensation adjustments, made to minimise overlap between the two fluorochromes. The cells were resuspended in  $1 \times$  binding buffer at a concentration of approximately  $1 \times 10^6$  cells per ml. Annexin V-FITC (5 μL) and Propidium Iodide (PI: 10 μL) solution were added to 500 μL of cell suspension. The cells were incubated for 10 min at room temperature and protected from light. After incubation the cells were analysed using a Beckman Coulter BD FACSCanto II flow cytometer emitting an excitation light at 488 nm from a laser. The detection was made at 518 nm for FITC detection and 620 nm for PI detection.

### MTT experiments

3-(4,5-Dimethylthiazol-2-yl)-2,5 diphenyltetrazoliumbromide (MTT) assay experiments were conducted following a protocol described by Mosmann.<sup>5</sup> MTT was used to titrate cell viability following drug treatment. HeLa cells were treated as described



for flow cytometry, whilst for Jurkat cells, doxorubicin was added to complete RPMI1640 to achieve final concentrations of 0.1, 0.3, 0.5 and 1  $\mu\text{M}$ . The cells were seeded at a density of  $3.6 \times 10^4$  cells per ml, 24 h after the previous passage to ensure exponential growth, and kept in T25 flasks in 5 ml of medium with the corresponding concentrations of doxorubicin. Following incubation for 8, 16, 32 and 48 h, the cells were centrifuged, the supernatant removed, and resuspended in 60  $\mu\text{L}$  of MTT: 10  $\mu\text{L}$  was plated per well in 6 wells (6 repeats) and incubated for 4 hours. Following incubation, tetrazolium crystals were dissolved in 100  $\mu\text{L}$  of DMSO. The absorbance intensity was measured by a microplate reader (VERSAmax) at 570 nm with a reference wavelength of 690 nm. Plates were read within 30 minutes of adding the DMSO. All experiments were performed in quadruplicate and the relative cell viability (%) was expressed as a percentage relative to the untreated control cells.

### Trypan blue experiments

20  $\mu\text{L}$  of cell suspension was mixed with 20  $\mu\text{L}$  of trypan blue 0.4% solution (Sigma-Aldrich, UK) in order to assess cell viability. The test was performed on a haemocytometer. The number of viable and non-viable cells in the haemocytometer were counted, and the viability percentage was calculated.

### IC<sub>50</sub> determination

In pharmacological research, the half maximal inhibitory concentration, IC<sub>50</sub>, is a common toxicity measure which indicates the concentration of a drug that is needed to inhibit a given biological process in half of the cells in a population. For chemotherapeutic agents that are cytotoxic, the IC<sub>50</sub> represents the concentration of the chemotherapeutic agent that is needed to inhibit population cell growth by half. The cytotoxicity of a compound is the extent to which that compound can damage the cell and this damage is dose dependent. Cytotoxic compounds can cause cell death in different ways including necrosis and apoptosis. The cytotoxicity can be determined by incubating cells with a range of concentrations of a drug for a period of time and quantifying the growth inhibition on the cells by comparing the viability of treated and healthy control. A dose response graph is typically used in which the effect of cell growth is plotted as a function of drug concentration. The Hill equation<sup>29</sup> has been widely used to describe the dose response relationship, in the 'sigmoid  $E_{\text{max}}$  model', given by:

$$E = \frac{E_{\text{max}}C^\alpha}{EC_{50}^\alpha + C^\alpha} \quad (3)$$

where  $E$  is the predicted effect of the drug,  $E_{\text{max}}$  is the maximum effect,  $C$  is the drug concentration,  $EC_{50}$  is the drug concentration for which 50% of the maximum effect is obtained and  $\alpha$  is the Hill coefficient of sigmoidicity.<sup>30</sup> For an inhibitory effect, values of  $\alpha$  are negative.

## Results and discussion

### Validation of DEP multiple subpopulation model against known mixtures of healthy and treated cells

It has previously been shown that when DEP analysis is performed on heterogeneous cell populations, the resulting DEP spectrum is the mathematical point-wise addition of the spectra of separate sub-populations.<sup>24,28</sup> Consequently, if the data are of sufficient quality, it is possible to model multiple populations by identifying separate dispersions and other characteristic features in the recorded spectrum. The accuracy of this is increased further where the populations can be characterised in advance.

We hypothesised that the data taken by the system presented here are sufficiently accurate for pair-wise modelling up to four populations, where the original populations have already been characterised. To test this, mean analyses ( $n = 15$ ) of Jurkat cells were analysed before and after 16 h of treatment with 10  $\mu\text{M}$  doxorubicin (referred to as healthy control and DOX-treated). Each analysis identified two populations: in the first case, the sample was found to contain 90% healthy cells and 10% which exhibited a significantly lower cytoplasmic capacitance, suggesting cell damage perhaps due to cell handling (ESI Fig. 1A†). Two populations were also found in the DOX-treated sample, one indicating apoptotic cells and the other presenting much smaller particles ( $\sim 1 \mu\text{m}$ ), suggested to be apoptotic bodies, in a 54 : 46% ratio (ESI Fig. 1B†). The two samples (HC and DOX) were then mixed in 25 : 75, 50 : 50 and 75 : 25 ratios and analysed with DEP using the average of five repeats. Analysis was performed by using best-fit software to estimate the ratios of the two established populations in which the spectra derived for the HC and DOX cells should be mixed in order to maximise the correlation coefficient. Ratios were estimated in 1% steps (and further 0.1% steps when necessary), with the highest  $R$  value selected. The results can be seen in Table 1; the system determined the ratios to an accuracy of 5% or better, with  $R$ -values  $\geq 0.98$  (and reaching up to 0.998). It was noted that the variability in the DEP replicates was increased for the treated sample indicating the heterogeneity of sample may not be as consistent as the two populations found in the healthy sample. This highlights the effectiveness of the system for the analysis of heterogeneous populations, such as for cytotoxicity analysis.

### IC<sub>50</sub> determination of doxorubicin on Jurkat cells by MTT, DEP and trypan blue

A common measurement of the efficacy of cellular assays is the determination of a response curve to a drug in order to determine its inhibitory concentration that affects 50% of cells, or IC<sub>50</sub>. Jurkat cells are electrophysiologically transformed by the use of anti-cancer drugs such as doxorubicin, thus DEP may present a rapid, simple-to-use and low-cost alternative to IC<sub>50</sub> assay techniques such as MTT or trypan blue. To determine the toxicity of doxorubicin on Jurkat cells, the percentage of viable cells after incubation with each concentration is needed. We incubated Jurkat cells for 8–32 h with



**Table 1** Untreated Healthy Control (100% HC) and DOX-treated (100% DOX) Jurkat cell populations ( $n = 15$ ), each determined to contain two sub-populations. The properties of these sub populations are given at the bottom of the table. These two treatment groups were mixed in known ratios ( $n = 7$ ) as indicated on left-hand column by the % of HC. Keeping DEP properties constant for the HC and DOX sub populations, the single-shell model was fitted iteratively in steps of 0.1% of each population combination. For each iteration the Pearson correlation coefficient ( $R$ ) was determined. The mixture % in each column indicates the ratio of HC and DOX sub populations which provided the best over-all fit. The totals of these best fit ratios can then be compared to the actual, known mixture (e.g. for the known 25% HC/75% DOX mixture, DEP best fit occurred at 30% HC/70% DOX)

		Best fit % with constant parameters						
		Healthy Control Total	Healthy Control (sub-pop 1)	Healthy Control (sub-pop 2)	DOX cells (sub-pop 3)	DOX fragments (sub-pop 4)	DOX total	$R$ value
Known mixture %	100% HC	100%	90%	10%	—	—	—	0.998
	75% HC	75.0%	67.5%	7.5%	13.5%	11.5%	25.0%	0.9908
	50% HC	55.0%	49.5%	5.5%	24.3%	20.7%	45.0%	0.9933
	25% HC	30.0%	27.0%	3.0%	37.8%	32.2%	70.0%	0.9742
	100% DOX	—	—	—	54%	46%	100%	0.9943
Cytoplasmic conductivity ( $S\ m^{-1}$ )			0.46	0.07	0.12	0.02		
Cytoplasmic relative permittivity			60	60	80	70		
Membrane conductance ( $S\ m^{-2}$ )			25.0	12.5	12.5	1.3		
Membrane capacitance ( $mF\ m^{-2}$ )			9.96	7.75	6.64	7.75		
Radius ( $\mu m$ )			6.5	6.0	5.5	1.0		

doxorubicin at concentrations between 0.1 to 1  $\mu M$ . After 8 h incubation with doxorubicin, in addition to the two populations similarly identified in ESI Fig. 1† for the healthy control, a third population had lower membrane capacitance and conductance and lower cytoplasmic conductivity and permittivity. The second population is interpreted as being affected by the drug but not dead, as the trypan blue test did not show that cells were necrotic.

After 16 h incubation with doxorubicin a fourth population, with properties indicating a small radius, was found; closer observation of the cells under the microscope confirmed the presence of cell fragments approximately 1–2  $\mu m$  in diameter. At each time point, the established DEP properties of these four populations were used to determine viability at each concentration (examples of this are shown in ESI Fig. 4† for 1  $\mu M$ ). This was performed through iterating sub population percentage, optimising  $R$  of the single shell fit to the spectra data. DEP viability % was interpreted as the total percentage of sub population 1 and 2. Again it was observed that the error associated with DEP replicates of the 32 h was higher than shorter incubation times suggesting the heterogeneity of the sample had increased. The effect of doxorubicin on Jurkat cells was also calculated by comparing the results at each concentration against the healthy control using both trypan blue and MTT, the results of which are shown in Table 3. For the lower concentration and shortened incubation times the MTT result was negative, indicating that those cells proliferated more than the healthy control. The numbers of trypan blue stained cells and unstained cells were also measured for each experiment, though this proved difficult at times when most of the cells were necrotic. There was a presence of ghost-like cells which were difficult to see under the microscope and appeared brighter than the rest or had a pale-blue appearance. For the

experiments with the longer incubation times and higher concentrations, the cell concentration appeared to be lower and the presence of very small debris was noticeable but difficult to quantify under the microscope.

The percentage of viable cells obtained using DEP, MTT and trypan blue, for each concentration at a given time point, was used to calculate the  $IC_{50}$  values with the Hill Model by fitting to a rectangular hyperbola with iterative least squares regression and error given is error of fit to data points using Kaleidagraph (Synergy Software, Reading, PA USA). Table 2 shows the  $IC_{50}$  values obtained with the different methods over time. Each DEP experiment results in a dielectrophoretic spectrum from which populations with different properties can be obtained. The healthy population is determined as a control and then after incubation with the drug, the healthy population (which consists of two sub populations) can be subtracted in order to obtain the properties of the remaining populations. In this study, the properties of the affected cells and cell fragments are assumed to be the same in all incubation time points and concentrations in order to obtain an estimate of their properties. The DEP results highlighted the presence of three populations after 8 h, as can be seen from the bend in the polarizability at higher frequencies, indicating a population with a lower membrane capacitance and cytoplasm conductivity. After 16 h a fourth population, made up of cell fragments, could be seen in the spectra. By 32 h, there was a noticeable decrease in the healthy populations of each concentration. The  $IC_{50}$  could be determined at this point and proved close to the result obtained with MTT at both 16 h and 24 h; it was also consistent with the value obtained by trypan blue at 32 h, though unlike DEP and MTT this method was unable to produce a result at 16 h.



**Table 2** Comparison of IC<sub>50</sub> of DOX on Jurkat cells using DEP, MTT and trypan blue. The growth inhibition was measured by MTT, whilst viability was measured by trypan blue, (*n* = 5) and DEP (*n* = 7) of Jurkat cells incubated with doxorubicin at different times. The viabilities For each treatment time, the responses at each concentration were used to calculate the IC<sub>50</sub> by fitting data to a rectangular hyperbola with iterative least squares regression; the error given is the error of fit to data points using KaleidaGraph (Synergy Software, Reading, PA USA)<sup>a</sup>

		0.1 μM	0.3 μM	0.5 μM	1 μM	IC <sub>50</sub>
DOX incubation time		MTT: growth inhibition (%)				
	8 h	-2.9 ± 0.013	-0.94 ± 0.014	2.7 ± 0.020	2.9 ± 0.026	0.37 ± 0.07
	16 h	3.0 ± 0.006	-1.0 ± 0.036	34.2 ± 0.019	56.1 ± 0.006	1.21 ± 0.20
	32 h	2.9 ± 0.019	50.5 ± 0.012	69.5 ± 0.003	79.5 ± 0.004	0.33 ± 0.04
		Trypan blue: % viability				
	8 h	94 ± 3	96 ± 2	98 ± 1	99 ± 1	DNC
	16 h	94 ± 3	97 ± 2	94 ± 1	82 ± 2	5.07 ± 0.75
	32 h	94 ± 3	60 ± 5	29 ± 1	27 ± 2	0.36 ± 0.035
		DEP: % viability (±1%)				
	8 h	90	94.5	83	85	0.14 ± 0.11
	16 h	90	85	65	20	0.70 ± 0.11
	32 h	90	40	35	0	0.25 ± 0.04

<sup>a</sup> DNC designates when Hill Model did not converge with given data.

### Cytotoxicity analysis of staurosporine on HeLa cells by MTT, DEP, Annexin-V and trypan blue

Staurosporine is a widely-used agent for the induction of apoptosis. To benchmark DEP against common methods of viability or apoptosis itself, HeLa cells were incubated with staurosporine and then DEP, flow cytometry, MTT and trypan blue measured at regular time-points.

The mean (*n* = 14) DEP spectra of HeLa cells, together with the modelled electrical parameters, are shown in ESI Fig. 2.† Analysis of the control HeLa population indicated that 15% of the population was small-radius debris, rising to 30% after 0.5 h incubation with staurosporine. After 0.5 h incubation with staurosporine the healthy population (population 1) had decreased by 18% and after 2 h by 41% compared to the healthy control. The mean cell radius had increased from 7.7 μm to 8.1 μm, coinciding with a decrease in cytoplasmic conductivity from 0.38 mS m<sup>-1</sup> to 0.26 mS m<sup>-1</sup> whilst the cytoplasmic permittivity remained the same. The membrane capacitance decreased from 38.7 mF m<sup>-2</sup> to 35.4 mF m<sup>-2</sup> whilst the membrane conductance remained constant. After 2 hours, cell debris accounted for 50% of the population, but the cell-sized population retained the cell properties as after 0.5 h, though the radius decreased to 7.26 μm (lower than the healthy control, but within the standard deviations). After 0.5 h incubation with staurosporine the healthy population (population 1) had decreased to 82% and after 2 h to 58%.

Flow cytometric analysis was performed for Propidium Iodide (PI) and Annexin V-FITC; the latter adheres to phosphatidylserine exposed on the cell membrane during early apoptosis, whilst PI indicates loss of membrane integrity in late apoptosis. In all experiments 10 000 events were measured, of which some fell outside the gating set by the control sample (ESI Fig. 3†). The healthy control showed a small percentage of early apoptotic cells, this could be because apoptosis can also be induced by cell stress. It also contained a small percentage of late apoptotic cells. After 0.5 h the healthy population decreased by 4% and the early apoptotic population increased by the same amount. The healthy population decreased as incubation time was longer. The late apoptotic population increased steadily as incubation time was longer.

The healthy control gated population was 77.4% of the events registered. The 0.5 h, 2 h, 4 h, 6 h, and 12 h gated populations were 75.3%, 59.8%, 42.5%, 37%, and 24.6% of the events registered, respectively. These results indicate that the presence of cell debris increases steadily from 0.5 h of incubation with 1 μM staurosporine. The viability determined by flow cytometry is shown in Table 3.

The viability of HeLa cells after each incubation time point was calculated by comparing their concentration against the healthy control concentration. Table 2 shows the results obtained with MTT. MTT was chosen in order to observe the viability of the cell population without harvesting methods

**Table 3** Comparison of HeLa cell viability after treatment with 1 μM staurosporine as measured by DEP (*n* = 14, ±SEM), trypan blue, flow cytometry, and MTT (*n* = 5, ±SEM)

		Viability (%) measured by method			
		Trypan blue	Flow cytometry	MTT viability	DEP
STS incubation time	Healthy control	92 ± 1	91 ± 3	100 ± 0	85 ± 5
	0.5 h	86 ± 3	87 ± 2	98 ± 1	70 ± 5
	2 h	75 ± 5	73 ± 6	92 ± 1	50 ± 5
	4 h	38 ± 1	27 ± 4	50 ± 1	0 ± 5



affecting the result. For the shorter incubation times the result is negative, indicating that those cells proliferated more than the healthy control. After 4 h ( $n = 5$ ) MTT shows that half of the population is still viable. For the healthy control the cell viability was 98%. The viabilities for the incubation time points were 98% at 0.5 h, 92% after 2 h, and 87% after 4 h.

The trypan blue experiments were carried out immediately before the DEP experiments in order to determine cell viability of the samples. The results, when compared with the flow cytometry populations that are not stained with PI correlate well, as seen in Table 3, indicating that DEP accords with flow cytometry in terms of cells with intact membranes. Previous results comparing DEP to other viability methods also showed DEP to underestimate viability when compared to trypan blue and flow cytometry, again suggesting DEP measures earlier apoptotic events than these methods resulting in a lower DEP viability measure. Confirmation of this could be found in this same study, where Nexin (which detects an early apoptotic feature of phosphatidylserine on the outer cell membrane) and DEP demonstrated near identical viability counts.<sup>16</sup> This is corroborated with another DEP study that showed a strong inverse relationship between PS externalisation and cytoplasmic conductivity.<sup>11</sup>

MTT overestimates the viability of the cells because during the early stages of apoptosis the cell is still able to metabolise the tetrazolium salt.<sup>5</sup> MTT on adherent cells was carried out whilst they were still attached to the microplate and, since no detachment was needed, the cells were not harmed by the harvesting process. The MTT experiments showed that the cells were viable from 0.5 h to 2 h. At 4 h, MTT estimated that half of the population was viable. When incubated in suspension, DEP detected a decrease in the healthy population after 0.5 h incubation, and that population also had lower cytoplasmic conductivity. The population had decreased to 80% (from 85% to 70%) and cytoplasm conductivity from 0.38 to 0.26 S m<sup>-1</sup>. Flow cytometry, for the 0.5 h sample, showed that the healthy population had decreased to 95% (from 91 to 87%). When the different methods are compared (Table 3) it is clear that the DEP result is comparable to both MTT and flow cytometry in terms of viability assessment, whilst being faster and substantially lower cost to implement.

DEP has previously been used to quantify apoptotic progression, detecting cells in early or late apoptosis from normal cells.<sup>7–20</sup> It can detect early events associated with the onset of apoptosis in a manner which can be correlated with other apoptotic events such as the activation of scramblases which translocate membrane phospholipids between inner and outer leaflets.<sup>11</sup> However, whilst tools for the study of apoptosis often focus on the analysis of the apoptotic process, a greater part of the analysis is in the quantification of the number of cells undergoing the phenomenon in order to determine the efficacy of drugs at different concentrations. This has been something that DEP has been previously unable to achieve, because the majority of DEP analysis methods use cell tracking in some form to measure the force on a population of cells. Cells in late apoptosis tend to break into small (>2 μm)

particles known as “apoptotic bodies” that are too small to track easily, making it difficult to quantify how many cells have entered this phase. The method described here uses a different approach, relying on the optical absorbance of cells within a well structure. Typically, 1000 cells will be contained within each well, with 20 wells being analysed. As cells disintegrate, they remain within the optical path and retain similar absorbance characteristics, allowing them to remain as part of the quantification process.

The multi-population model used here used four fixed models for healthy cells plus those in apoptosis, tracking the variation in population sizes by finding the best-fit proportions of the four populations. The fits to the four curves were typically determined to have values of  $R^2 > 0.99$  and, when mixed in fixed ratios, were accurate to within 5% of the actual population ratios. When using these models to track actual cell populations undergoing apoptosis there is good agreement between DEP and the other methods. For Jurkat cells, results with DEP typically produced a lower value by a factor of ~2; given that IC<sub>50</sub> values typically deal with orders of magnitude, this is functionally a very similar result. For HeLa cells where the assay operated on much shorter timescales, DEP produced a result much more rapidly than the other methods, principally because DEP measures cell stress rather than cell death, by identifying ion efflux early in the apoptotic process, though MTT did start to show similar results some 2 h later.

Taken together, these results suggest that DEP can be used as an effective tool for quantifying cell death. It produces IC<sub>50</sub> results comparable to standard assays such as MTT, flow cytometry, and trypan blue. The technique does not require any cell staining, is faster than the other methods, producing functionally similar results with significantly lower complexity and operating cost and has demonstrated sensitivity to physiological changes in cells across early to late stage apoptosis.

## Competing interests

KFH and MPH are directors of DEPtech Ltd, which produce the 3DEP instrument used here.

## Acknowledgements

Funding for this work was provided from the South East of England Development Agency and Finance South East. A studentship to RMTS was provided by Labtech International.

## References

- 1 M. M. Martinez, R. D. Reif and D. Pappas, *Anal. Methods*, 2010, 2, 996–1004.
- 2 V. A. Fadok, D. R. Voelker, P. A. Campbell, J. J. Cohen, D. L. Bratton and P. M. Henson, *J. Immunol.*, 1992, 148, 2207–2216.





- 3 G. Koopman, C. P. M. Reutelingsperger, G. A. M. Kuijten, R. M. J. Keehnen, S. T. Pals and M. H. J. Vanoers, *Blood*, 1994, **84**, 1415–1420.
- 4 M. van Engeland, F. C. Ramaekers, B. Schutte and C. P. Reutelingsperger, *Cytometry*, 1996, **24**, 131–139.
- 5 T. Mosmann, *J. Immunol. Methods*, 1983, **65**, 55–63.
- 6 G. Ormerod, *Flow Cytometry: A Practical Approach*, OUP Oxford, 2000.
- 7 S. Chin, M. P. Hughes, H. M. Coley and F. H. Labeed, *Int. J. Nanomed.*, 2006, **1**, 333–337.
- 8 X. J. Wang, F. F. Becker and P. R. C. Gascoyne, *Biochim. Biophys. Acta*, 2002, **1564**, 412–420.
- 9 F. H. Labeed, H. M. Coley and M. P. Hughes, *Biochim. Biophys. Acta, Gen. Subj.*, 2006, **1760**, 922–929.
- 10 L. Duncan, H. Shelmerdine, M. P. Hughes, H. M. Coley, Y. Hübner and F. H. Labeed, *Phys. Med. Biol.*, 2008, **53**, N1–N7.
- 11 H. J. Mulhall, A. Cardnell, K. F. Hoettges, F. H. Labeed and M. P. Hughes, *Integr. Biol.*, 2015, **7**, 1396–1401.
- 12 R. Pethig and M. S. Talary, *IET Nanobiotechnol.*, 2007, **1**, 2–9.
- 13 S. J. Martin, C. P. Reutelingsperger, A. J. McGahon, J. A. Rader, R. C. van Schi, D. M. Laface and D. T. Green, *J. Exp. Med.*, 1995, **341**, 1545–1556.
- 14 C. D. Bortner and J. A. A. Cidowski, *Philos. Trans. R. Soc.*, 2014, **369**, 1638.
- 15 C. J. Huang, A. L. Chen, L. Wang, M. Guo and J. Yu, *Biomed. Microdevices*, 2007, **9**, 335–343.
- 16 M. Nikolic-Jaric, T. Cabel, E. Salimi, A. Bhide, K. Braasch, M. Butler, G. E. Bridges and D. J. Thomson, *Biomicrofluidics*, 2013, **7**, 024101.
- 17 D. Lee, B. Hwang, Y. Choi and B. Kim, *Sens. Actuators, A*, 2016, **242**, 1–8.
- 18 D. Lee and B. Kim, *Int. J. Precis. Eng. Man.*, 2015, **16**, 609–613.
- 19 K. Braasch, M. Nikolic-Jaric, T. Cabel, E. Salimi, G. E. Bridges, D. J. Thomson and M. Butler, *Biotechnol. Bioeng.*, 2013, **110**, 2902–2914.
- 20 R. T. Kalyana Kumar, S. Liu, J. D. Minna and S. Prasad, *Biochim. Biophys. Acta*, 2016, **1860**, 1877–1883.
- 21 C. H. Fry, S. C. Salvage, A. Manazza, E. Dupont, F. H. Labeed, M. P. Hughes and R. I. Jabr, *Biophys. J.*, 2012, **103**, 2287–2294.
- 22 S. Mahabadi, F. H. Labeed and M. P. Hughes, *Electrophoresis*, 2015, **36**, 1493–1498.
- 23 Y. Hübner, K. F. Hoettges, G. E. N. Kass, S. L. Ogin and M. P. Hughes, *IEEE Proc. Bionanotechnol.*, 2005, **4**, 21–25.
- 24 K. F. Hoettges, Y. Hübner, L. M. Broche, S. L. Ogin, G. E. N. Kass and M. P. Hughes, *Anal. Chem.*, 2008, **80**, 2063–2068.
- 25 L. M. Broche, K. F. Hoettges, S. L. Ogin, G. E. N. Kass and M. P. Hughes, *Electrophoresis*, 2011, **32**, 2393–2399.
- 26 A. Irimajiri, T. Hanai and A. Inouye, *J. Theor. Biol.*, 1979, **78**, 251–269.
- 27 U. Lei, P. H. Sun and R. Pethig, *Biomicrofluidics*, 2011, **5**, 044109.
- 28 L. M. Broche, F. H. Labeed and M. P. Hughes, *Phys. Med. Biol.*, 2005, **50**, 2267–2274.
- 29 S. Goutelle, M. Maurin, F. Rougier, X. Barbaut, L. Bourguignon, M. Ducher and P. Maire, *Fundam. Clin. Pharmacol.*, 2008, **22**, 633–648.
- 30 A. V. Hill, *J. Physiol.*, 1910, **40**(suppl.), iv–vii.

